Journal of Chemical Crystallography
https://doi.org/10.1007/s10870-020-00849-y

ORIGINAL PAPER

Reactions of $[Os_3(CO)_{10}(\mu\text{-}H)_2]$ and $[Os_3(CO)_8\{\mu_3\text{-}Ph_2PCH_2P(Ph)C_6H_4\}(\mu\text{-}H)]$ with pymS−$SnPh_3$ (pymS = pyrimidine-2-thiolate): Synthesis and Structure of Triosmium Clusters Containing pymS Ligand

Md Tuhinur R. Joy[1] · Shishir Ghosh[1] · Shariff E. Kabir[1]

Received: 11 October 2019 / Accepted: 7 July 2020

Abstract

Reactivity of pymS−$SnPh_3$ (pymS = pyrimidine-2-thiolate) towards two unsaturated triosmium clusters $[Os_3(CO)_{10}(\mu\text{-}H)_2]$ and $[Os_3(CO)_8\{\mu_3\text{-}Ph_2PCH_2P(Ph)C_6H_4\}(\mu\text{-}H)]$ are investigated. Reaction of pymS−$SnPh_3$ with $[Os_3(CO)_{10}(\mu\text{-}H)_2]$ affords $[Os_3(CO)_{10}(\mu\text{-}pymS)(\mu\text{-}H)]$ (**1**) and $[Os_3(CO)_9(\mu_3\text{-}pymS)(\mu\text{-}H)]$ (**2**), while with $[Os_3(CO)_8\{\mu_3\text{-}Ph_2PCH_2P(Ph)C_6H_4\}(\mu\text{-}H)]$ leads to the isolation of only $[Os_3(CO)_8(\mu\text{-}pymS)(\mu\text{-}H)(\mu\text{-}dppm)]$ (**3**). In both reactions, the products are formed via incorporation of the thiolate part (pymS) of pymS−$SnPh_3$ into the parent clusters through Sn−S bond cleavage. Clusters **1**–**3** have been characterized by a combination of analytical and spectroscopic data together with single crystal X-ray diffraction analysis.

Graphic Abstract

Reactions of pymS−$SnPh_3$ with two unsaturated triosmium clusters have been investigated which resulted in the isolation and characterization of three triosmium clusters containing a pymS ligand.

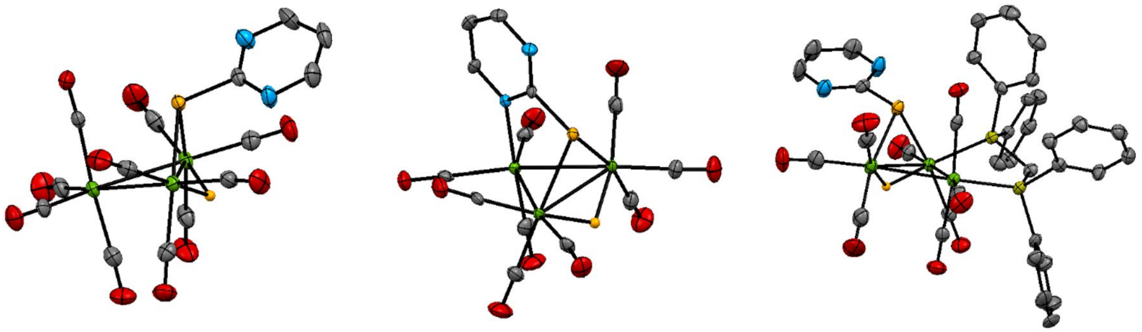

Keywords Osmium · Carbonyls · Pyrimidine-2-thiolate · Tin-sulfur bond cleavage · Crystal structure

Introduction

Over the past four decades, transition metal complexes containing heterocyclic-thiolate ligands have drawn considerable attention owing to their structural diversity [1–13], biological relevance [14–17] and potential as precursor for binary metal-sulfide materials employed in the semiconductor industry [18–21]. Consequently, the reactivity of these heterocyclic thiols towards various transition metal centers has been widely investigated [1–13, 22–41]. Recently, we have initiated a research program in our laboratory with the aim of incorporating tin or germanium into the coordination sphere of transition metal clusters together with heterocyclic thiolate ligands since both tin [42–45] and germanium [46–48] are widely used as modifiers to control the reactivity and selectivity of transition-metal catalysts. To achieve this

---

✉ Shishir Ghosh
sghosh_006@yahoo.com

✉ Shariff E. Kabir
skabir_ju@yahoo.com

[1] Department of Chemistry, Jahangirnagar University, Savar, Dhaka 1342, Bangladesh

in one step we have used ligands that possess both functionalities such as pyS−SnPh$_3$ (py = pyridine-2-thiolate) and pymS−SnPh$_3$ (pym = pyrimidine-2-thiolate) [49–51]. For example, the reaction of pyS−SnPh$_3$ with [Ru$_3$(CO)$_{12}$] afforded diruthenium [Ru$_2$(CO)$_6$(SnPh$_3$)$_2$(μ-pyS)] as the major product together with a small amount of tetraruthenium [Ru$_4$(CO)$_{12}$(SnPh$_3$)(μ$_3$-pyS)], while the reaction with [Os$_3$(CO)$_{10}$(NCMe)$_2$] yielded only triosmium [Os$_3$(CO)$_9$(SnPh$_3$)(μ$_3$-pyS)] [51] (Scheme 1). Unsaturated [Os$_3$(CO)$_8${μ$_3$-PPh$_2$CH$_2$P(Ph)C$_6$H$_4$}(μ-H)] also reacted with pyS−SnPh$_3$ to give [Os$_3$(CO)$_8$(μ-pyS)(μ-dppm)(μ-H)] and the Os-Sn bimetallic cluster [Os$_3$(CO)$_7$(SnPh$_3$){μ-Ph$_2$PCH$_2$P(Ph)C$_6$H$_4$}(μ-pyS)(μ-H)] [51] (Scheme 2).

As part of our investigation on bimetallic Os–Sn clusters containing heterocylic thiolate ligand(s), we have now investigated the reactions of unsaturated [Os$_3$(CO)$_{10}$(μ-H)$_2$] and [Os$_3$(CO)$_8${μ$_3$-Ph$_2$PCH$_2$P(Ph)C$_6$H$_4$}(μ-H)] with pymS−SnPh$_3$. Unfortunately, these reactions do not furnish any bimetallic Os–Sn clusters, but lead to the isolation of products formed via incorporation of only the heterocyclic thiolato part of the ligand into these clusters. The details of these reactions are described in this article.

Experimental Section

Materials and Methods

Unless otherwise noted, all reactions were carried out under a nitrogen atmosphere using standard Schlenk techniques. Reagent grade solvents were dried by the standard methods and were freshly distilled prior to use. [Os$_3$(CO)$_{12}$] was purchased from Strem Chemicals, Inc. and used without further purification. Bis(diphenylphosphino)methane (dppm), pyrimidine-2-thiol (pymSH) and triphenyltin chloride (Ph$_3$SnCl) were purchased from Sigma-Aldrich and used as received. The precursor compounds [Os$_3$(CO)$_{10}$(μ-H)$_2$] [52], [Os$_3$(CO)$_8${μ$_3$-Ph$_2$PCH$_2$P(Ph)C$_6$H$_4$}(μ-H)] [53] and pymS−SnPh$_3$ [54, 55] were prepared according to the literature. Infrared spectra were recorded on a Shimadzu IR Prestige-21 spectrophotometer, while NMR spectra were recorded on a Bruker Avance III HD (400 MHz) instrument. All chemical shifts are reported in δ units and are referenced to the residual protons of the deuterated solvents (^{1}H) and to external 85% H$_3$PO$_4$ (^{31}P). Elemental analyses were performed by the Microanalytical Laboratories of the Wazed Miah Science Research Centre at Jahangirnagar University. Products were

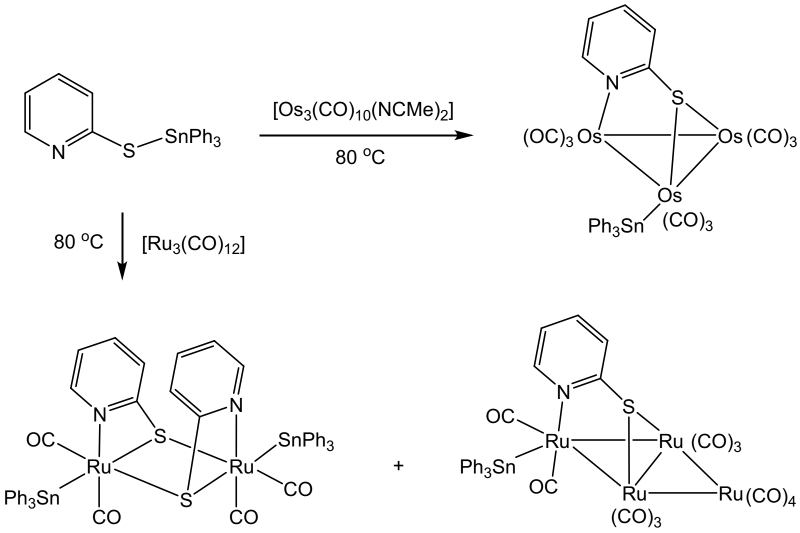

Scheme 1 Reactions of [Os$_3$(CO)$_{10}$(NCMe)$_2$] and [Ru$_3$(CO)$_{12}$] with pyS−SnPh$_3$

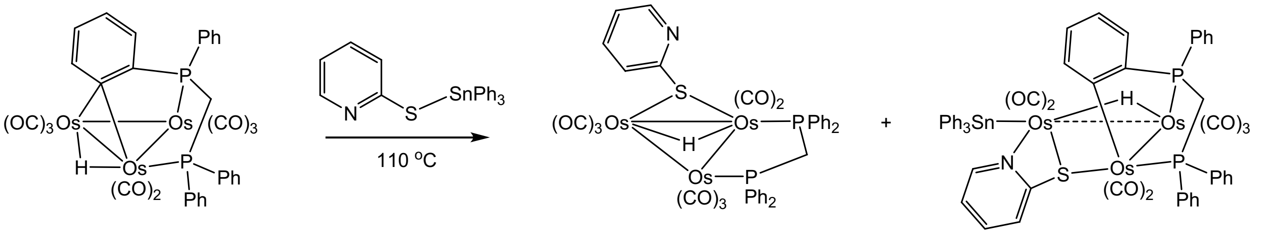

Scheme 2 Reaction of [Os$_3$(CO)$_8${μ$_3$-Ph$_2$PCH$_2$P(Ph)C$_6$H$_4$}(μ-H)] with pyS−SnPh$_3$

separated in the air by TLC plates coated with 0.25 mm of silica gel (HF254-type 60, E. Merck, Germany).

Reaction of $[Os_3(CO_{10}(\mu\text{-}H)_2]$ with pymS−$SnPh_3$

To a CH_2Cl_2 solution (15 ml) of $[Os_3(CO)_{10}(\mu\text{-}H)_2]$ (50 mg, 0.059 mmol) was added pymS−$SnPh_3$ (27 mg, 0.059 mmol) and the reaction mixture was stirred at room temperature for 24 h. The solvent was removed under reduced pressure and the resulting residue chromatographed by TLC on silica gel. Elution with cyclohexane/CH_2Cl_2 (7:3 v/v) developed three bands. The first band was unreacted $[Os_3(CO)_{10}(\mu\text{-}H)_2]$ (trace), while the second and third bands afforded $[Os_3(CO)_{10}(\mu\text{-pymS})(\mu\text{-}H)]$ (**1**) (25 mg, 44%) isolated as yellow crystals and $[Os_3(CO)_9(\mu_3\text{-pymS})(\mu\text{-}H)]$ (**2**) (19 mg, 35%) isolated as red crystals, respectively, after recrystallization from *n*-hexane/CH_2Cl_2 at 4 ºC.

Data for **1** Anal. Calc. for $C_{14}H_4N_2O_{10}Os_3S$: C, 17.46; H, 0.42; N, 2.91. Found: C, 17.78; H, 0.48; N, 3.01%. IR (ν(CO), hexane): 2110 w, 2070 vs, 2062 s, 2023 vs, 2018s, 2008 s, 1987 w cm^{-1}. ^{1}H NMR ($CDCl_3$): δ 8.65 (d, J 4.8 Hz, 2H), 7.15 (t, J 4.8 Hz, 1H), – 17.18 (s, 1H).

Data for **2** Anal. Calc. for $C_{13}H_4N_2O_9Os_3S$: C, 16.70; H, 0.43; N, 3.00. Found: C, 16.97; H, 0.47; N, 3.05%. IR (ν(CO), CH_2Cl_2): 2087 w, 2058 vs, 2029 vs, 2000 m, 1950 w cm^{-1}. ^{1}H NMR ($CDCl_3$): δ 9.23 (dd, J 4.8, 2.4 Hz, 1H), 8.55 (dd, J 4.8, 2.4 Hz, 1H), 7.15 (t, J 4.8 Hz, 1H), – 15.03 (s, 1H).

Thermolysis of $[Os_3(CO)_{10}(\mu\text{-pymS})(\mu\text{-}H)]$ (1) at 128 ºC

An *n*-octane solution (10 mL) of **1** (20 mg, 0.021 mmol) was heated to reflux for 4 h. The solvent was removed under reduced pressure and the residue chromatographed by TLC on silica gel. Elution with cyclohexane/CH_2Cl_2 (7:3 v/v) developed three bands. The first band was unreacted **1** (trace), while the third band afforded **2** (12 mg, 62%). The content of the second band was too small for complete characterization.

Reaction of $[Os_3(CO)_8\{\mu_3\text{-}Ph_2PCH_2P(Ph)C_6H_4\}(\mu\text{-}H)]$ with pymS−$SnPh_3$

To a toluene solution (15 mL) of $[Os_3(CO)_8\{\mu_3\text{-}Ph_2PCH_2P(Ph)C_6H_4\}(\mu\text{-}H)]$ (50 mg, 0.042 mmol) was added pymS−$SnPh_3$ (20 mg, 0.043 mmol) and the reaction mixture was heated to reflux for 1 h. The reaction mixture was then allowed to cool to room temperature. The solvent was removed under reduced pressure and the residue chromatographed by TLC on silica gel. Elution with cyclohexane/CH_2Cl_2 (1:1, v/v) developed four bands. The third band was unreacted $[Os_3(CO)_8\{\mu_3\text{-}Ph_2PCH_2P(Ph)C_6H_4\}(\mu\text{-}H)]$ (trace), while the fourth band afforded $[Os_3(CO)_8(\mu\text{-pymS})(\mu\text{-}H)(\mu\text{-dppm})]$ (**3**) (17 mg, 31%) isolated as yellow crystals after recrystallization from *n*-hexane/CH_2Cl_2 at 4 ºC. The content of the first and second bands was too small for complete characterization.

Data for **3**: Anal. Calc. for $C_{37}H_{26}N_2O_8Os_3P_2S$: C, 34.41; H, 2.03; N, 2.17. Found: C, 34.75; H, 2.11; N, 2.23%. IR (ν(CO), CH_2Cl_2): 2071 s, 2025 s, 1996 vs, 1955 w, 1927 w cm^{-1}. ^{1}H NMR ($CDCl_3$): δ 8.54 (d, J 4.8 Hz, 1H), 7.72 (m, 2H), 7.56 (d, J 2.4 Hz, 4H), 7.48 (m, 7H), 7.37 (m, 4H), 7.31(m, 2H), 7.16 (m, 2H), 6.99 (t, J 4.8 Hz, 1H), 5.97 (m, 1H), 4.38 (m, 1H), – 16.01 (d, J 30.4 Hz, 1H). ^{31}P{^{1}H} NMR ($CDCl_3$): δ – 25.2 (d, J 44 Hz, 1P), – 26.8 (d, J 44 Hz, 1P).

Crystal Structure Determination

Single crystals of **1**–**3** suitable for X-ray diffraction analyses were grown by slow diffusion of *n*-hexane into a CH_2Cl_2 solution of each compound at 4 ºC. Crystals were mounted on a nylon loop and diffraction data collected on a Bruker APEX-III CCD diffractometer at low temperatures (see Table 1) using Mo-Kα radiation ($\lambda = 0.71073$ Å). Unit cell determination, data reduction and integration were carried out with SAINT + [56], and absorption corrections were applied using the program SADABS [57]. The structures were solved with the ShelXS [58] structure solution program by direct methods and refined by full-matrix least-squares on the basis of F^2 using ShelXL [59] within the OLEX2 [60] graphical user interface. All non-hydrogen atoms were refined anisotropically and the hydrogen atoms (except for the hydrides) were included using a riding model. Pertinent crystallographic parameters are given in Table 1.

Results and Discussion

Reaction of $[Os_3(CO_{10}(\mu\text{-}H)_2]$ with pymS−$SnPh_3$

The room temperature reaction between $[Os_3(CO)_{10}(\mu\text{-}H)_2]$ and pymS−$SnPh_3$ led to the formation of two new triosmium clusters $[Os_3(CO)_{10}(\mu\text{-pymS})(\mu\text{-}H)]$ (**1**) and $[Os_3(CO)_9(\mu_3\text{-pymS})(\mu\text{-}H)]$ (**2**) in 44 and 35% yield, respectively, after usual chromatographic separation and workup (Scheme 3). Both **1** and **2** are formed by coordination of pymS to the parent cluster via Sn−S bond cleavage of pymS−$SnPh_3$ with apparent elimination of Ph_3SnH. Formation of **2** in this room temperature reaction is unexpected since removal of a carbonyl from the remote osmium in **1** should require moderate heating under normal circumstances. In a separate experiment, we indeed found that **1** does not convert to **2** at room temperature, but requires heating in boiling *n*-octane (128 °C). This observation indicates that **1** is not a precursor of **2** in this reaction, and they are

Table 1 Crystal data and structure refinement details for **1**–**3**

Compound	**1**	**2**	**3**
CCDC	1,954,927	1,954,928	1,954,929
Empirical formula	$C_{21}H_6N_3O_{15}Os_{4.5}S_{1.5}$	$C_{13}H_4N_2O_9Os_3S$	$C_{37}H_{26}N_2O_8Os_3P_2S$
Formula weight	1444.28	934.84	1291.20
Temperature (K)	193(1)	193(1)	210(1)
Wavelength (Å)	0.71073	0.71073	0.71073
Crystal system	Orthorhombic	Monoclinic	Monoclinic
Space group	*Pnma*	*P2₁/c*	*P2₁*
Unit cell dimensions			
a (Å)	12.344(5)	8.971(4)	11.669(5)
b (Å)	37.421(14)	11.710(5)	28.103(10)
c (Å)	13.270(5)	17.687(9)	12.038(5)
α (°)	90	90	90
β (°)	90	93.031(18)	106.671(13)
γ (°)	90	90	90
Volume (Å^3)	6130(4)	1855.4(15)	3782(3)
Z	8	4	4
Density (calculated) (Mg/m^3)	3.130	1855.4(15)	2.268
Absorption coefficient (mm^{-1})	18.766	20.657	10.248
F(000)	5112	1648	2400
Crystal size (mm^3)	0.238 × 0.169 × 0.091	0.151 × 0.101 × 0.078	0.354 × 0.113 × 0.043
2θ range for data collection (°)	4.354 to 52.222	4.546 to 54.352	4.57 to 56.806
Index ranges	$-15 \leq h \leq 15$	$-11 \leq h \leq 11$	$-15 \leq h \leq 15$
	$-46 \leq k \leq 46$	$-14 \leq k \leq 15$	$-37 \leq k \leq 37$
	$-16 \leq l \leq 16$	$-22 \leq l \leq 22$	$-15 \leq l \leq 16$
Reflections collected	179,029	23,138	73,199
Independent reflections [R_{int}]	6153 [$R_{int} = 0.0543$]	4101 [$R_{int} = 0.0614$]	18,825 [$R_{int} = 0.0321$]
Data/restraints/parameters	6153/0/432	4101/0/258	18,825/1/964
Goodness of fit on F^2	1.199	1.122	0.988
Final R indices [$I > 2\sigma(I)$]	$R_1 = 0.0189$, $wR_2 = 0.0355$	$R_1 = 0.0208$, $wR_2 = 0.0476$	$R_1 = 0.0229$, $wR_2 = 0.0316$
R indices (all data)	$R_1 = 0.0213$, $wR_2 = 0.0361$	$R_1 = 0.0231$, $wR_2 = 0.0484$	$R_1 = 0.0324$, $wR_2 = 0.0332$
Largest diff. peak and hole (e. Å^{-3})	0.92 and − 1.82	1.40 and − 1.65	0.88 and − 0.71

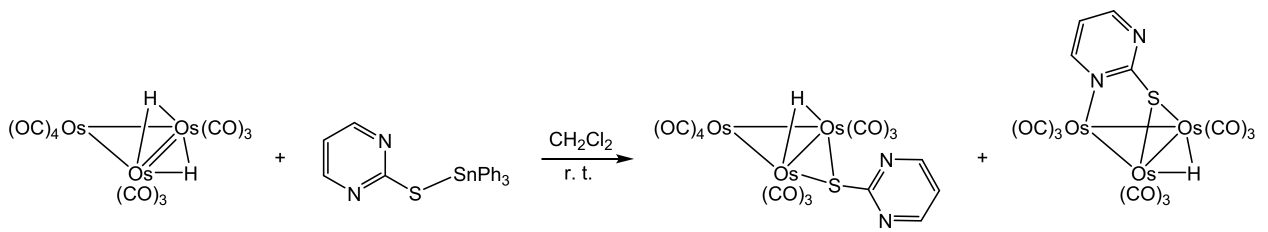

1

2

Scheme 3 Reaction of $[Os_3(CO)_{10}(\mu\text{-}H)_2]$ with pymS−SnPh$_3$

formed following different pathways. We also assume that the tin moiety of the ligand most probably plays a role in facilitating the formation of **2** in this reaction. Both new clusters have been characterized by elemental and spectroscopic data in addition to single crystal X-ray diffraction analyses.

The solid-state molecular structure of **1** is depicted in Fig. 1 with the caption containing selected bond distances and angles. The molecule contains an isosceles triangle of osmium atoms [Os(1)–Os(2) 2.8623(9) Å, Os(1)–Os(3) 2.8637(10) Å and Os(2)–Os(3) 2.8381(8) Å] coordinated by ten carbonyls, an edge bridging pymS ligand and a hydride.

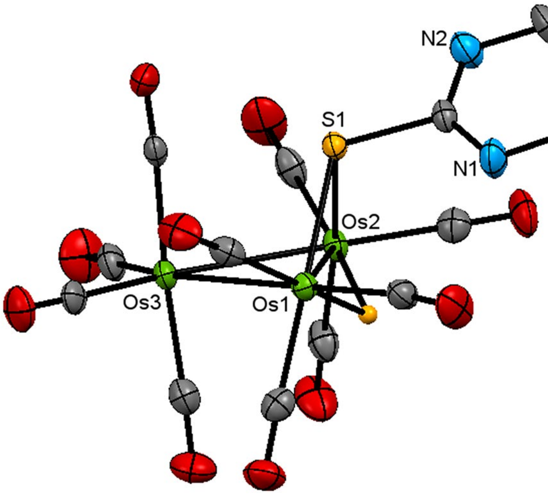

Fig. 1 Molecular structure of $[Os_3(CO)_{10}(\mu\text{-pymS})(\mu\text{-H})]$ (**1**) showing 50% probability atomic displacement ellipsoids. Pyrimidine ring hydrogen atoms are omitted for clarity. Selected bond lengths (Å) and bond angles (°): Os(1)–Os(2) 2.8623(9), Os(1)–Os(3) 2.8637(10), Os(2)–Os(3) 2.8381(8), Os(1)–S(1) 2.4094(15), Os(2)–S(1) 2.4211(13), Os(2)–Os(1)–Os(3) 59.425(10), Os(1)–Os(2)–Os(3) 60.313(18), Os(1)–Os(3)–Os(2) 60.26(3), S(1)–Os(1)–Os(2) 53.85(3), S(1)–Os(1)–Os(3) 81.48(3), Os(1)–S(1)–Os(2) 72.68(3)

The pymS ligand bridges the Os(1)–Os(2) edge through the sulfur atom and the Os–S bond distances [Os(1)–S(1) 2.4094(15) Å and Os(2)–S(1) 2.4211(13) Å] are similar to those observed for related clusters [32–41, 51, 61–63]. The hydride was located from the difference map and refined; it was found to span across the same Os–Os edge bridged by the pymS ligand. Both Os(1) and Os(2) are bound to three carbonyls, while the remote osmium, Os(3) is coordinated by four carbonyls. The gross structural features of **1** are akin to those of its pyridine-2-thiolate (pyS) and 4,6-dimethylpyrimidine-2thiolate (Me_2pymS) analogues $[Os_3(CO)_{10}(\mu\text{-pyS})(\mu\text{-H})]$ [61] and $[Os_3(CO)_{10}(\mu\text{-Me}_2\text{pymS})(\mu\text{-H})]$ [63], respectively. The solution spectroscopic data of **1** are consistent with the solid-state structure. The IR spectrum exhibits several absorption bands between 2110 and 1987 cm^{-1} indicating the presence of only terminal carbonyls in the molecule, whilst the ^{1}H NMR spectrum displays a doublet at δ 8.65 and a triplet at δ 7.15 (J 4.8 Hz) with an intensity ratio of 2:1 due to the pyrimidine ring protons together with an upfield singlet at $\delta - 17.18$ for the edge bridging hydride.

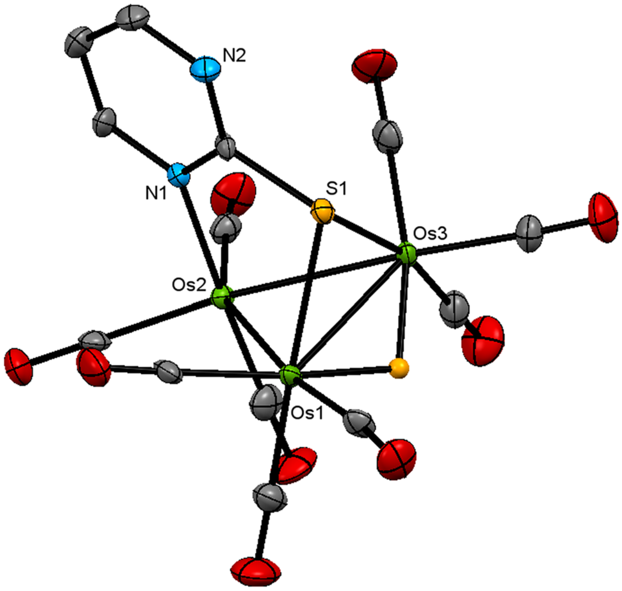

Fig. 2 Molecular structure of $[Os_3(CO)_9(\mu\text{-pymS})(\mu\text{-H})]$ (**2**) showing 50% probability atomic displacement ellipsoids. Pyrimidine ring hydrogen atoms are omitted for clarity. Selected bond lengths (Å) and bond angles (°): Os(1)–Os(2) 2.7953(9), Os(1)–Os(3) 2.8537(9), Os(2)–Os(3) 2.8012(13), Os(2)–N(1) 2.167(4), Os(1)–S(1) 2.4233(13), Os(3)–S(1) 2.4290(16), Os(2)–Os(1)–Os(3) 59.44(3), Os(1)–Os(2)–Os(3) 61.316(15), Os(1)–Os(3)–Os(2) 59.240(17), S(1)–Os(1)–Os(3) 54.07(4), S(1)–Os(1)–Os(2) 80.81(4), Os(1)–S(1)–Os(3) 72.05(4), N(1)–Os(2)–Os(1) 88.35(10)

Figure 2 shows the solid-state molecular structure of **2** and its caption contains selected bond distances and angles. The cluster core consists of an isosceles triangle of osmium atoms [Os(1)–Os(2) 2.7953(9) Å, Os(1)–Os(3) 2.8537(9) Å and Os(2)–Os(3) 2.8012(13) Å] which is ligated by nine carbonyls, a capping pymS and an edge bridging hydride. The carbonyls are evenly distributed between three osmium atoms. The pymS ligand lies almost perpendicular to the metallic plane by bridging the longest Os–Os edge through the sulfur atom, while coordinating to the third osmium using one of the ring nitrogen atoms. The Os–N [Os(2)–N(1) 2.167(4) Å] and Os–S [Os(1)–S(1) 2.4233(13) Å and Os(3)−S(1) 2.4290(16) Å] bond distances are very similar to those found in related clusters [32–41, 51, 61–63]. The hydride ligand was located from the structural analysis, which also bridges the longest Os–Os edge, but lies on the opposite side of the metallic plane with respect to the pymS ligand. The spectroscopic data of **2** suggest that the solid-state structure persists in solution. The IR spectrum shows five absorption bands within the range 2110–1987 cm^{-1} for the nine terminal carbonyls, while the ^{1}H NMR spectrum displays an upfield singlet at $\delta - 15.03$ for the bridging hydride together with two doublet of doublets and a triplet at δ 9.23 (J 4.8, 2.4 Hz), 8.55 (J 4.8, 2.4 Hz) and 7.15 (J 4.8 Hz), respectively, for the pyrimidine ring protons which are in accord with the solid-state structure.

Reaction of $[Os_3(CO)_8\{\mu_3\text{-}Ph_2PCH_2P(Ph)C_6H_4\}(\mu\text{-H})]$ with pymS−$SnPh_3$

Unlike $[Os_3(CO)_{10}(\mu\text{-H})_2]$, the unsaturated $[Os_3(CO)_8\{\mu_3\text{-}Ph_2PCH_2P(Ph)C_6H_4\}(\mu\text{-H})]$ did not react with pymS−$SnPh_3$ at room temperature and required heating in boiling toluene, which resulted in the formation of [$Os_3(CO)_8$(μ-pymS)(μ-H)(μ-dppm)] (**3**) in 31% yield (Scheme 4). Cluster **3** is formed by incorporation of only the heterocyclic thiolato part of the ligand and the tin part is most probably eliminated as $Ph_3Sn(C_6H_4CH_3)$ or Ph_3SnOH, since formation of **3** also requires an additional hydrogen atom, which we assume is abstracted from the solvent toluene molecule or adventitious water during the reaction. In a separate experiment, we heated **3** in boiling *n*-octane in order to coordinate one of the pyrimidine ring nitrogen atoms to the cluster core, but we could not isolate any product from this thermal reaction, which only led to slow decomposition of **3**. Cluster **3** was earlier reported from the room temperature reaction between [$Os_3(CO)_8${$μ_3$-$Ph_2PCH_2P(Ph)C_6H_4$}(μ-H)] and pyrimidine-2-thiol (pymSH) and was characterized by analytical and spectroscopic data [64]. Now we have carried out a single crystal X-ray diffraction analysis for **3** the results of which are summarized in Fig. 3.

The molecular structure of **3** is very similar to that of its thiophenolate analog [$Os_3(CO)_8$(μ-SPh)(μ-H)(μ-dppm)] [65]. The molecule comprises a triosmium core with three slightly different Os–Os interactions [Os(1)–Os(2) 2.8602(9) Å, Os(1)–Os(3) 2.8743(11) Å and Os(2)–Os(3) 2.8494(9) Å]. Eight carbonyls, a dppm, a pymS and a hydride complete the coordination sphere of the cluster. The carbonyls are distributed in such a way that both Os(1) and Os(2) are bonded to three, while Os(3) is coordinated to two. The dppm ligand acts in bridging capacity and spans the shortest Os–Os edge. The pymS and hydride ligands bridge the longest Os–Os edge simultaneously, lying on the opposite face of the metallic plane with respect to each other. The Os–P [Os(2)–P(1) 2.3237(19) Å and Os(3)–P(1) 2.3150(18) Å] and Os − S [Os(1)–S(1) 2.4041(18) Å and Os(3)–S(1) 2.4153(17) Å] bond distances are very similar to those observed in [$Os_3(CO)_8$(μ-SPh)(μ-H)(μ-dppm)] [65] and other related clusters [32–41, 51, 61–63]. The solution spectroscopic data of **3** are in accord with the solid-state structure. The ^{1}H NMR spectrum displays an upfield singlet at $\delta - 16.01$ for the bridging hydride and two multiplets at δ 5.97 and 4.38, each integrating to one proton, attributed to the methylene protons of the dppm ligand. The spectrum also displays a series of multiplets in the aromatic region for the phenyl and pyrimidyl ring protons, whilst the $^{31}P\{^1H\}$ NMR spectrum exhibits two equally intense doublets at $\delta - 25.2$ and $- 26.8$ (J 44 Hz) for the phosphorus atoms of the dppm ligand.

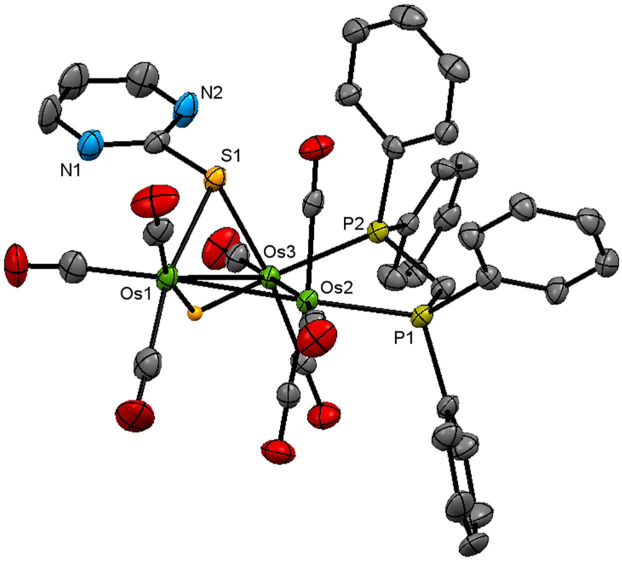

Fig. 3 Molecular structure of [$Os_3(CO)_8$(μ-pymS)(μ-H)(μ-dppm)] (**3**) showing 50% probability atomic displacement ellipsoids. Hydrogen atoms except the bridging hydride ligand are omitted for clarity. Selected bond lengths (Å) and bond angles (°): Os(1)–Os(2) 2.8602(9), Os(1)–Os(3) 2.8743(11), Os(2)–Os(3) 2.8494(9), Os(2)–P(1) 2.3237(19), Os(3)–P(1) 2.3150(18), Os(1)–S(1) 2.4041(18), Os(3)–S(1) 2.4153(17), Os(2)–Os(1)–Os(3) 59.59(3), Os(1)–Os(2)–Os(3) 60.453(19), Os(1)–Os(3)–Os(2) 59.959(16), S(1)–Os(1)–Os(3) 53.57(4), S(1)−Os(1)−Os(2) 81.46(4), Os(1)–S(1)–Os(3) 73.23(5), P(1)–Os(2)–Os(3) 92.53(4), P(1)−Os(2)−Os(3) 152.91(4)

Conclusions

The reactions of pymS−$SnPh_3$ with two unsaturated triosmium clusters [$Os_3(CO)_{10}(μ-H)_2$] and [$Os_3(CO)_8${$μ_3$-$Ph_2PCH_2P(Ph)C_6H_4$}(μ-H)] have been investigated which led to the isolation of two new triosmium clusters [$Os_3(CO)_{10}$(μ-pymS)(μ-H)] (**1**) and [$Os_3(CO)_9$($μ_3$-pymS)(μ-H)] (**2**) and the previously reported [$Os_3(CO)_8$(μ-pymS)(μ-H)(μ-dppm)] [64]. These clusters are apparently formed

Scheme 4 Reaction of [$Os_3(CO)_8${$μ_3$-$Ph_2PCH_2P(Ph)$ C_6H_4}(μ-H)] with pymS−$SnPh_3$

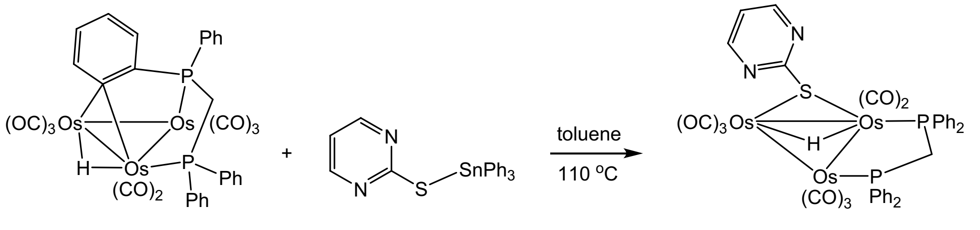

3

via Sn−S bond cleavage of the pymS−SnPh$_3$ ligand followed by incorporation of the heterocyclic thiolate moiety into the parent clusters. The pymS ligand acts in edge bridging capacity in **1** and **3**, while it caps a face of the metal triangle in **2**. The fate of the tin moiety remains unknown from the present study. Although the reactions of ArS−EPh$_3$ (E = Sn, Ge) ligands with polynuclear transition metal centers usually afford products containing both thiolate and EPh$_3$ moieties [51, 66], isolation of products containing only the thiolate or EPh$_3$ part from this type of reactions is rare but not unprecedented [49, 50, 65]. For example, we have earlier reported that a similar reaction between the unsaturated [Os$_3$(CO)$_8${μ$_3$-Ph$_2$PCH$_2$P(Ph)C$_6$H$_4$}(μ-H)] and PhS−GePh$_3$ does not lead to the isolation of any cluster bearing both PhS and Ph$_3$Ge moieties, but afforded [Os$_3$(CO)$_8$(μ-SPh)(μ-H)(μ-dppm)] and [Os$_3$(CO)$_7$(μ-SPh)(μ-SC$_6$H$_4$)(μ-H)(μ-dppm)] containing only the thiolate part of the ligand [65].

Supplementary Data

Crystallographic data for the structural analyses have been deposited with the Cambridge Crystallographic Data centre. CCDC 1,954,927, CCDC 1,954,928 and CCDC 1,954,929 contain supplementary crystallographic data for compound **1**, **2** and **3** respectively. These data can be obtained free of charge from the Director, CCDC, 12 Union Road, Cambridge, CB2 1 EZ, UK (fax: + 44-1223-336,033; Email: deposit@ccdc.cam.ac.uk or www: https://www.ccdc.ac.uk).

Acknowledgements Financial support from the Ministry of Science and Technology, the Government of the People's Republic of Bangladesh (SG and SEK) is acknowledged. We also thank the Wazed Miah Science Research Center, Jahangirnagar University, Bangladesh for providing some technical facilities required for this work.

References

1. Choi N, Conole G, Kessler M, King JD, Mays MJ, McPartlin M, Pateman GE, Solan GA (1999) J Chem Soc Dalton Trans 22:3941–3948
2. Cockerton B, Deeming AJ, Karim M, Hardcastle KI (1991) J Chem Soc Dalton Trans 431–437
3. Deeming AJ, Karim M, Powell NI, Hardcastle KI (1990) Polyhedron 9:623–626
4. Deeming AJ, Hardcastle KI, Meah MN, Bates PA, Dawes HM, Hursthouse MB (1988) J Chem Soc Dalton Trans 1:227–233
5. Deeming AJ, Karim M, Powell NI (1990) J Chem Soc Dalton Trans 2321–2324.
6. Kole GK, Vivekananda KV, Kumar M, Ganguly R, Deya S, Jain VK (2015) CrystEngComm 17:4367–4376
7. Tyagi A, Kole GK, Shah AY, Wadawale A, Srivastava AP, Kumar M, Kedarnath G, Jain VK (2019) J Organomet Chem 887:24–31
8. Lugan N, Bonnet JJ, Ibers JA (1985) J Am Chem Soc 107:4484–4491
9. Johnson BFG, Lewis J, Pippard DA (1981) J Chem Soc Dalton Trans 2:407–412
10. Rosenfield SG, Swedberg SA, Arora SK, Mascharak PK (1986) Inorg Chem 25:2109–2114
11. Rose DJ, Chang YD, Chen Q, Zubieta J (1994) Inorg Chem 23:5167–5168
12. Kitagawa S, Munakata M, Shimono H, Matsuyama S, Masuda S (1990) J Chem Soc Dalton Trans 7:2105–2109
13. Deeming AJ, Karim M, Bates PA, Hursthouse MB (1988) Polyhedron 7:1401–1403
14. Katiyar D, Tiwari VK, Tripathi RP, Srivastava A, Chaturvedi V, Srivastava R, Srivastava BS (2003) Bioorg Med Chem 11:4369–4375
15. Kienitz CO, Thöne C, Jones P (1996) Inorg Chem 35:3990–3997
16. Castro R, Durán ML, Garcia-Vázquez JA, Romero J, Sousa A, Castiñeiras A, Hiller W, Strähle J (1990) J Chem Soc Dalton Trans 2:531–534
17. Rosenfield SG, Berends HP, Gelmini L, Stephan DW, Mascharak PK (1987) Inorg Chem 26:2792–2797
18. Lee J, Emge TJ, Brennan JG (1997) Inorg Chem 36:5064–5068
19. Cheng Y, Emge TJ, Brennan JG (1996) Inorg Chem 35:342–346
20. Berardini M, Brennan J (1995) Inorg Chem 34:6179–6185
21. Rose DJ, Chang YD, Chen Q, Kettler PB, Zubieta J (1995) Inorg Chem 34:3973–3979
22. Kabir SE, Hogarth G (2009) Coord Chem Rev 253:1285–1315
23. Kabir SE, Ahmed F, Ghosh S, Mamun RA, Haworth DT, Lindeman SV, Siddiquee TA, Bennett DW (2009) J Chem Crystallogr 39:595–602
24. Rahman MS, Sarker JC, Ghosh S, Kabir SE (2012) Aust J Chem 65:796–801
25. Hoque A, Islam S, Karim M, Ghosh S, Hogarth G (2015) Inorg Chem Commun 54:69–72
26. Chowdhury MAH, Rajbangshi S, Karim M, Ghosh S, Kabir SE, Siddiquee TA, Nesterov VN, Richmond MG (2015) Inorg Chim Acta 434:97–103
27. Ahmad MF, Sarker JC, Azam KA, Kabir SE, Ghosh S, Hogarth G, Siddiquee TA, Richmond MG (2013) J Organomet Chem 728:30–37
28. Haque MR, Ghosh S, Hogarth G, Richmond MG, Kabir SE (2015) Inorg Chim Acta 434:150–157
29. Moni MR, Ghosh S, Mobin SM, Tocher DA, Hogarth G, Richmond MG, Kabir SE (2018) J Organomet Chem 871:167–177
30. Abedin SMT, Haque MR, Ghosh S, Tocher DA, Richmond MG, Kabir SE (2019) Polyhedron 164:55–63
31. Ghosh S, Kabir SE, Pervin S, Hossain GMG, Haworth DT, Lindeman SV, Siddiquee TA, Bennett DW, Roesky HW (2009) Z Anorg Allg Chem 635:76–87
32. Ghosh S, Kabir SE, Pervin S, Raha AK, Hossain GMG, Haworth DT, Lindeman SV, Bennett DW, Siddiquee TA, Salassa L, Roesky HW (2009) Dalton Trans 18:3510–3518
33. Kabir SE, Alam J, Ghosh S, Kundu K, Hogarth G, Tocher DA, Hossain GMG, Roesky HW (2009) Dalton Trans 23:4458–4467
34. Ghosh S, Khanam KN, Hossain MK, Hossain GMG, Haworth DT, Lindeman SV, Hogarth G, Kabir SE (2010) J Organomet Chem 695:1146–1154
35. Ghosh S, Khanam KN, Hossain GMG, Haworth DT, Lindeman SV, Hogarth G, Kabir SE (2010) New J Chem 34:1875–1884
36. Ghosh S, Camellia FK, Fatema K, Hossain MI, Al-Mamum MR, Hossain GMG, Hogarth G, Kabir SE (2011) J Organomet Chem 696:2935–2942
37. Ghosh S, Mia MSA, Begum E, Hossain GMG, Kabir SE (2012) Inorg Chim Acta 384:76–82
38. Moni MR, Mia MJ, Ghosh S, Tocher DA, Mobin SM, Siddiquee TA, Kabir SE (2018) Polyhedron 146:154–160
39. Abedin SMT, Moni MR, Ghosh S, Tocher DA, Hossain GMG, Mobin SM, Kabir SE (2018) Polyhedron 152:164–171

40. Ghosh S, Kabir SE, Khatun M, Haworth DT, Lindeman SV, Siddiquee TA, Bennett DW (2009) J Chem Crystallogr 39:632–637
41. Khaleque MA, Azam KA, Karim MM, Ghosh S, Hogarth G, Kabir SE (2012) Aus J Chem 65:773–778
42. Holt MS, Wilson WL, Nelson JH (1989) Chem Rev 89:11–49
43. Coupé JN, Jordão E, Fraga MA, Mendes MJ (2000) Appl Catal A 199:45–51
44. Santos SM, Silva AM, Jordao E, Fraga MA (2004) Catal Commun 5:377–381
45. Toba M, Tanaka S, Niwa S, Mizukami F, Koppany Z, Guczi L, Cheah K-Y, Tang T-S (1999) Appl Catal A 189:243–250
46. Lafaye G, Micheaud-Especel C, Montassier C, Marecot P (2002) Appl Catal A 230:19–30
47. Didillon B, Candy JP, Lepepetier F, Ferretti OA, Basset JM (1993) Stud Surf Sci Catal 78:147–154
48. Lafaye G, Mihut C, Especel C, Marecot P, Amiridis MD (2004) Langmuir 20:10612–10616
49. Al-Mamun MR, Ghosh S, Kabir SE, Sarker JC, Hogarth G, Nicholson BK (2015) J Coord Chem 68:1903–1912
50. Ghosh S, Pervin R, Raha AK, Kabir SE, Nicholson BK (2009) Inorg Chim Acta 362:4226–4230
51. Raha AK, Ghosh S, Hossain I, Kabir SE, Nicholson BK, Hogarth G, Salassa L (2011) J Organomet Chem 696:2153–2160
52. Sappa E, Valle M (1977) Inorg Synth 26:365–369
53. Clucas JA, Foster DF, Harding MM, Smith AK (1984) J Chem Soc Chem Commun 14:949–950
54. Abel EW, Brady DB (1965) J Chem Soc 1192–1197
55. Pollar RC (1970) The chemistry of organotin compounds. Logos Press, London
56. Bruker, SAINT (8.37A), Bruker AXS Inc., Madison (2015)
57. Bruker, SADABS-2014/5, Bruker AXS Inc., Madison (2014)
58. Sheldrick GM (2008) Acta Crystallogr Sect A 64:112–122
59. Sheldrick GM (2015) Acta Cryst C71:3–8
60. Dolomanov OV, Bourhis LJ, Gildea RJ, Howard JAK, Puschmann H (2009) J Appl Crystallogr 42:339–341
61. Ainscough EW, Brodie AM, Coll RK, Waters JM (1999) Aust J Chem 52:801–806
62. Au Y-K, Cheung K-K, Wong W-K (1995) J Chem Soc Dalton Trans 1047–1057
63. Au Y-K, Cheung K-K, Wong W-K (1995) Inorg Chim Acta 228:267–275
64. Kabir SE, Malik KMA, Molla E, Mottalib MA (2000) J Organomet Chem 616:157–164
65. Raha AK, Ghosh S, Kabir SE, Nicholson BK, Tocher DA (2009) J Organomet Chem 694:752–756
66. Kabir SE, Raha AK, Hassan MR, Nicholson BK, Rosenberg E, Sharmin A, Salassa L (2008) Dalton Trans 32:4212–4219